

Article

Correlations between [⁶⁸Ga]Ga-DOTA-TOC Uptake and Absorbed Dose from [¹⁷⁷Lu]Lu-DOTA-TATE

Ragnar Bruvoll ^{1,2}, Johan Blakkisrud ¹, Lars Tore Mikalsen ^{1,3}, James Connelly ¹  and Caroline Stokke ^{1,2,*} ¹ Division of Radiology and Nuclear Medicine, Oslo University Hospital, 0424 Oslo, Norway² Department of Physics, University of Oslo, 0315 Oslo, Norway³ Department of Life Sciences and Health, Oslo Metropolitan University, 0130 Oslo, Norway

* Correspondence: carsto@ous-hf.no

Simple Summary: Peptide receptor radionuclide therapy (PRRT) with [¹⁷⁷Lu]Lu-DOTA-TATE is used to treat gastroenteropancreatic neuroendocrine tumours (GEP-NET) by targeting somatostatin receptors (SSTRs) found on the cell surface. High SSTR expression on [⁶⁸Ga]Ga-DOTA-TOC PET/CT decides patient eligibility. This study aimed to investigate potential correlations between therapeutic absorbed dose to tumours and pre-therapeutic [⁶⁸Ga]Ga-DOTA-TOC uptake, and found that the [⁶⁸Ga]Ga-DOTA-TOC PET imaging may predict the [¹⁷⁷Lu]Lu-DOTA-TATE uptake to a certain extent. However, there could be a high variance between predicted and actual absorbed doses for individual patients.

Abstract: Purpose: The aim of this paper was to investigate correlations between pre-therapeutic [⁶⁸Ga]Ga-DOTA-TOC uptake and absorbed dose to tumours from therapy with [¹⁷⁷Lu]Lu-DOTA-TATE. Methods: This retrospective study included 301 tumours from 54 GEP-NET patients. The tumours were segmented on pre-therapeutic [⁶⁸Ga]Ga-DOTA-TOC PET/CT, and post-therapy [¹⁷⁷Lu]Lu-DOTA-TATE SPECT/CT images, using a fixed 40% threshold. The SPECT/CT images were used for absorbed dose calculations by assuming a linear build-up from time zero to day one, and mono-exponential wash-out after that. Both SUV_{mean} and SUV_{max} were measured from the PET images. A linear absorbed-dose prediction model was formed with SUV_{mean} as the independent variable, and the accuracy was tested with a split 70–30 training-test set. Results: Mean SUV_{mean} and SUV_{max} from [⁶⁸Ga]Ga-DOTA-TOC PET was 24.0 (3.6–84.4) and 41.0 (6.7–146.5), and the mean absorbed dose from [¹⁷⁷Lu]Lu-DOTA-TATE was 26.9 Gy (2.4–101.9). A linear relationship between SUV_{mean} and [¹⁷⁷Lu]Lu-DOTA-TATE activity concentration at 24 h post injection was found ($R^2 = 0.44$, $p < 0.05$). In the prediction model, a root mean squared error and a mean absolute error of 1.77 and 1.33 Gy/GBq, respectively, were found for the test set. Conclusions: There was a high inter- and intra-patient variability in tumour measurements, both for [⁶⁸Ga]Ga-DOTA-TOC SUVs and absorbed doses from [¹⁷⁷Lu]Lu-DOTA-TATE. Depending on the required accuracy, [⁶⁸Ga]Ga-DOTA-TOC PET imaging may estimate the [¹⁷⁷Lu]Lu-DOTA-TATE uptake. However, there could be a high variance between predicted and actual absorbed doses.

Keywords: peptide receptor radionuclide therapy; [⁶⁸Ga]Ga-DOTA-TOC; PET/CT; [¹⁷⁷Lu]Lu-DOTA-TATE; SPECT/CT; dosimetry; prediction model



Citation: Bruvoll, R.; Blakkisrud, J.; Mikalsen, L.T.; Connelly, J.; Stokke, C. Correlations between [⁶⁸Ga]Ga-DOTA-TOC Uptake and Absorbed Dose from [¹⁷⁷Lu]Lu-DOTA-TATE. *Cancers* **2023**, *15*, 1134. <https://doi.org/10.3390/cancers15041134>

Academic Editor: David Wong

Received: 29 December 2022

Revised: 1 February 2023

Accepted: 7 February 2023

Published: 10 February 2023



Copyright: © 2023 by the authors. Licensee MDPI, Basel, Switzerland. This article is an open access article distributed under the terms and conditions of the Creative Commons Attribution (CC BY) license (<https://creativecommons.org/licenses/by/4.0/>).

1. Introduction

Gastroenteropancreatic neuroendocrine tumours (GEP-NET) are heterogeneous malignancies, characterised by a variable expression of somatostatin receptors (SSTR) on the cell surface of the dispersed neuroendocrine system in the pancreas and other parts of the gastrointestinal tract [1–3]. Peptide receptor radionuclide therapy (PRRT) is a molecular cancer treatment using SSTR to target GEP-NETs. A high uptake of a diagnostic somatostatin analogue (SSTA) in tumour lesions is a common measure of PRRT eligibility [4,5].

^{68}Ga -DOTA-labelled SSTAs are currently considered the preferred tool for patient evaluation of SSTR expression [6–9], and, for example, the PET tracer [^{68}Ga]Ga-DOTA-TOC has shown favourable performance and is commonly used [10].

Several radiolabelled SSTA alternatives, such as [^{111}In]In-DOTA-TOC, [^{111}In]In-octreotide, [^{90}Y]Y-DOTA-TOC, [^{177}Lu]Lu-DOTA-NOC, [^{177}Lu]Lu-DOTA-TATE, and [^{177}Lu]Lu-DOTA-TOC, have been applied for therapeutic use [8,11–15]. PRRT with [^{177}Lu]Lu-DOTA-TATE delivers targeted radiation and has shown promising response and survival statistics [15,16], while additionally permitting post-treatment imaging and personalised dosimetry [17]. [^{177}Lu]Lu-DOTA-TATE is usually prescribed by multiple cycles of 7.4 GBq with intervals of eight weeks between [15]. Based on post-therapy SPECT/CT measurements of activity concentration at various time points, absorbed dose calculations can be performed. Dosimetry can be used for treatment optimisation, by limiting absorbed dose to organs at risk, and should ideally be performed for tumours as well as to monitor the absorbed dose to the target tissue. A high inter- and intra-patient variability in tumour-absorbed doses from PRRT is commonly observed [18–20], emphasising the need for personalised treatment. Given a sufficiently correlated uptake, the absorbed dose from PRRT with [^{177}Lu]Lu-DOTA-TATE could potentially be predicted from measurements of [^{68}Ga]Ga-DOTA-TOC. While the two radiopharmaceuticals are based on similar peptides, differences in SSTR affinity between TOC and TATE have been observed *in vitro*, although the clinical consequences of these differences remain uncertain [21]. In comparisons of tumour uptake of [^{68}Ga]Ga-DOTA-TOC and [^{68}Ga]Ga-DOTA-TATE as a tool for staging and PRRT patient selection, only minor clinical implications were shown [10,22]. [^{177}Lu]Lu-DOTA-TATE has been found to have a 2.1 longer residence time in tumours than [^{177}Lu]Lu-DOTA-TOC [23], indicating that, opposed to the uptake level, the pharmacokinetics vary. Still, these comparisons are not directly translatable to predict correlations between [^{68}Ga]Ga-DOTA-TOC and [^{177}Lu]Lu-DOTA-TATE, as the radionuclide can possibly also change the molecular behaviour. A few earlier studies have investigated the correlation between PET-derived [^{68}Ga]Ga-DOTA-TOC uptake and SPECT-derived [^{177}Lu]Lu-DOTA-TATE uptake [24], and one study also investigated and found potential for absorbed dose prediction [25].

The aim of this work was to explore the correlation between [^{68}Ga]Ga-DOTA-TOC SUV and [^{177}Lu]Lu-DOTA-TATE uptake parameters in the first of the standard 7.4 GBq treatment fractions for tumours, and to investigate an absorbed dose prediction model for the therapy based on pre-therapeutic [^{68}Ga]Ga-DOTA-TOC PET/CT scans.

2. Materials and Methods

2.1. Patient Population

This study included 54 consecutive patients diagnosed with metastatic and progressive or recurrent GEP-NET, treated with at least one fraction of [^{177}Lu]Lu-DOTA-TATE PRRT. Eligibility criteria for the treatment were radiologic, symptomatic or biochemical progression despite optimal conventional treatment, and a high expression of SSTR as assessed on [^{68}Ga]Ga-DOTA-TOC PET/CT scans. Histological sampling was performed prior to the treatment to establish tumour grade and Ki-67 index. Adequate hepatic, renal and hematologic function are also critical prerequisites for treatment.

2.2. Image Acquisition

Pre-therapeutic PET/CT imaging (example in Figure 1A,C) was performed on a GE Discovery MI, 78 min (range: 54–96 min) post administration a nominal, fixed, activity dosage of 150 MBq [^{68}Ga]Ga-DOTA-TOC for patients above 35 years old. The acquisition time was 100 s per bed with 50% overlap. The images were gated using the Varian trigger system and reconstructed in the expiratory phase (Q.Static). The images were reconstructed with a Bayesian penalised likelihood reconstruction (Q.Clear) with a beta factor of 500, on a 384×384 matrix of 1.82 mm pixels with a slice thickness of 2.79 mm. The CT scans were acquired at 120 kV and a dose modulation noise index of 34.5 and reconstructed with an

iterative reconstruction (ASIR-V) with 40% filtering on 512×512 matrices. The pixel size was 0.84 mm with slice thickness 0.625 mm.

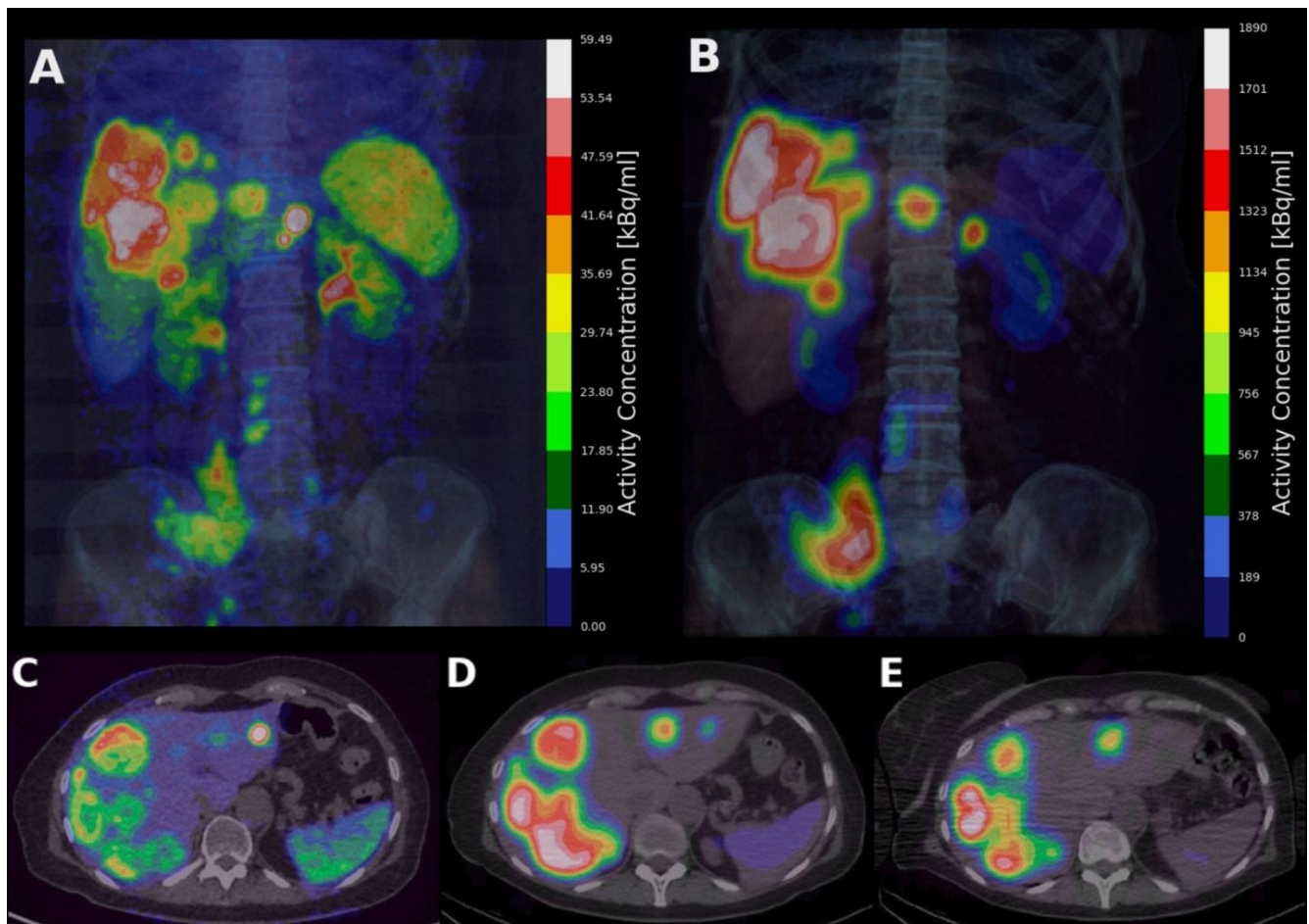


Figure 1. Maximum intensity projection (MIP) of a $[^{68}\text{Ga}]\text{Ga-DOTA-TOC}$ PET/CT image (A); and corresponding $[^{177}\text{Lu}]\text{Lu-DOTA-TATE}$ SPECT/CT image at the 24 h p.i. timepoint (B); axial slices of $[^{68}\text{Ga}]\text{Ga-DOTA-TOC}$ (C); and $[^{177}\text{Lu}]\text{Lu-DOTA-TATE}$ at t_{24} (D); and t_{168} (E), showing uptake in SSTR-expressing tumours. Physiologic uptake in kidneys, spleen and liver is also visible.

$[^{177}\text{Lu}]\text{Lu-DOTA-TATE}$ SPECT/CT imaging (example in Figure 1B,D,E) was on average performed 23.1 h (range 21.0–26.8) and 167.0 h (range 119.1–218.8 h) post administration (t_{24} and t_{168} , respectively) of the first treatment cycle for all patients. An additional image (t_4) on average 4.7 h (range 3.4–6.5) was acquired for nine of the patients. The average administered activity was 7574 MBq (range 7247–7907 excl. one patient given 4195 MBq). The imaging was performed on a GE Discovery 670 NM/CT scanner with a medium energy, general purpose collimator. The images were acquired with an energy window set at 208 keV \pm 10% with 120 projections of 30 s frame duration, and two adjacent scatter windows of \pm 5%. A scatter- and attenuation-corrected reconstruction with four iterations and eight subsets without resolution recovery was performed with the vendor software (Xeleris, GE Healthcare). Matrix size was 128×128 and isotropic voxels of 4.42 mm were reconstructed. The CT scans were acquired at 120 kV and a dose modulation noise index of 26 and reconstructed with an iterative reconstruction (ASIR) with 40% filtering on 512×512 matrices. The pixel size was 0.98 mm with slice thickness 2.5 mm.

2.3. $[^{68}\text{Ga}]\text{Ga-DOTA-TOC}$ PET Measurements

Tumours which could be visually matched between all images (PET and SPECT at t_{24} and t_{168}), with negligible overlap with adjacent activity sources, were included for analysis.

A manual identification of tumours confirmed by a nuclear medicine specialist was followed by a fixed threshold method for measurements, using a threshold of 40% [24] of the SUV_{max} . Both SUV_{max} , SUV_{mean} , and the volume defined by the threshold, referred to as the somatostatin receptor expressing tumour volume (SRETV) from here on, were recorded.

2.4. [^{177}Lu]Lu-DOTA-TATE SPECT Measurements and Tumour Dosimetry

The tumours were delineated using 40% threshold determined by volume matching in a phantom study, from which recovery coefficients were also found (Supplementary Figure S1). The VOI-derived counts were converted to activity by a system specific calibration coefficient of 8.4 cps/MBq. Time-activity curves (TACs) were calculated by assuming a linear activity build-up from time of administration to the first measuring point (t_{24}), followed by a mono-exponential curve fit based on t_{24} and t_{168} . The TAC was integrated to yield the time-integrated activity (\tilde{A}). The tumour mass (m) was estimated by measuring the volume at t_{24} and assuming a tissue mass density of 1 g/mL. The absorbed dose was calculated by assuming local deposition and a dose factor $DF = 0.0853 \text{ Gy}\cdot\text{g}/\text{MBq}\cdot\text{h}$, including all non-penetrative radiation from ^{177}Lu reported in the ICRP 2008 publication [26]. The activity concentrations at each time point, $A_{conc,4h}$, $A_{conc,24h}$, and $A_{conc,168h}$ were also calculated and normalised for injected amount of activity to the individual patient for some of the analyses.

$$D = \frac{\tilde{A}}{m} DF \quad (1)$$

2.5. Prediction Analyses

A linear estimator between [^{68}Ga]Ga-DOTA-TOC SUV_{mean} and [^{177}Lu]Lu-DOTA-TATE absorbed dose per administered activity (D/A_{adm}) was used.

$$D/A_{adm} = SUV_{mean} \cdot \alpha + \beta \quad (2)$$

Here α and β are fitting parameters.

To test the performance of the predictive model, the patients were split into a 70–30 training (37 patients, 210 tumours) test (17 patients, 91 tumours) set. The root mean squared error the mean absolute error and the coefficient of determination (R^2) were calculated for the test set based on fitting parameters found from the training set.

The prediction model was further explored by testing the ability to classify the tumour absorbed dose as higher or lower than the population median using logistic regression and receiver operating characteristics curves.

2.6. Group Analysis

Differences in absorbed dose and differences between predicted and actual absorbed dose were investigated for multiple tumour groups. Tumours were grouped by anatomical site (hepatic, lymphatic and skeletal lesions were compared), SUV-parameters and tumour mass. Two approaches were explored; one where tumours were divided into groups of equal size, and one where equal range of the parameter were grouped. The group differences of relative error between predicted and measured absorbed dose were tested with a one-way analysis of variance (ANOVA)-test and significance of individual group differences were conducted using the Tukey-test. The difference of absorbed dose between groups was also tested.

2.7. Statistics

A Shapiro–Wilk normality test and visual inspection of the probability plots of the residues were performed to test for normality. Pearson correlation was performed to test linear correlation between parameters. The linear correlation was evaluated in terms of the coefficient of determination, R^2 . Mean absolute error and root mean squared error were also used to score model performance. A significance level of 0.05 was used. All statistical analyses were conducted with the SciPy statistical functions module and the

Sklearn library, both in Python 3.8 (Python Software Foundation, Wilmington, DE, USA). The probability plot of the residuals was created with the SciPy stats probplot function against the normal distribution.

3. Results

3.1. Patient Characteristics and Tumour Parameters

This study included 54 patients (15 female, 39 male) with an average age of 65 years (range 38–82 years). A total of 301 tumours (1–15 per patient, 3 being most frequent) were analysed, the majority being hepatic (230/301) or lymphatic (35/301). The [⁶⁸Ga]Ga-DOTA-TOC and [¹⁷⁷Lu]Lu-DOTA-TATE parameters are included in Table 1 and Figure 2.

Table 1. Mean and standard deviation of parameters measured in all 301 tumours from [⁶⁸Ga]Ga-DOTA-TOC PET/CT and [¹⁷⁷Lu]Lu-DOTA-TATE SPECT/CT images.

| | Total | Training Dataset | Test Dataset |
|--|---------------|------------------|---------------|
| Characteristic | | | |
| Number of patients | 54 | 37 | 17 |
| Number of tumours | 301 | 210 | 91 |
| PET parameters | | | |
| Mean ± Standard deviation | | | |
| SUV _{mean} | 24.0 ± 14.5 | 24.1 ± 15.1 | 23.7 ± 12.9 |
| SUV _{max} | 41.0 ± 24.9 | 41.2 ± 26.0 | 40.7 ± 22.2 |
| SRETV [mL] | 29.4 ± 45.9 | 31.1 ± 49.8 | 25.5 ± 35.5 |
| SPECT parameters | | | |
| Mean ± Standard deviation | | | |
| Absorbed dose [Gy] | 26.9 ± 15.1 | 26.6 ± 15.1 | 27.6 ± 15.2 |
| Absorbed dose/A _{adm} [Gy/GBq] | 3.6 ± 2.0 | 3.5 ± 2.0 | 3.8 ± 2.0 |
| A _{conc,4} /A _{adm} [(kBq/mL)/GBq] * | 224.8 ± 113.1 | 220.0 ± 92.3 | 235.1 ± 151.3 |
| A _{conc,24} /A _{adm} [(kBq/mL)/GBq] | 262.3 ± 148.4 | 256.2 ± 148.2 | 276.3 ± 148.7 |
| A _{conc,168} /A _{adm} [(kBq/mL)/GBq] | 99.0 ± 58.7 | 96.7 ± 60.4 | 104.2 ± 54.4 |
| Effective half-life after t ₂₄ [hours] | 105.7 ± 24.5 | 106.3 ± 23.7 | 104.3 ± 26.3 |
| Tumour mass [g] | 45.8 ± 81.8 | 45.3 ± 73.6 | 47.1 ± 98.5 |

* Not all patients underwent imaging at this time point, and only 57 tumours are represented by this number.

3.2. Correlation between [⁶⁸Ga]Ga-DOTA-TOC and [¹⁷⁷Lu]Lu-DOTA-TATE Parameters for the Full Data Set

The absorbed dose had a strong linear correlation to A_{conc,24} (R² = 0.82, p < 0.05) but not to the effective half-life after 24 h (R² = 0.04, p < 0.05) (Figure 3). SUV_{mean} and SUV_{max} were strongly correlated (R² = 0.98, p < 0.05). A linear correlation was found between SUV and A_{conc,4}/A_{adm} (SUV_{mean}: R² = 0.57, p < 0.05, SUV_{max}: R² = 0.53, p < 0.05). A somewhat weaker correlation was observed between SUV and A_{conc,24}/A_{adm} (SUV_{mean}: R² = 0.44, p < 0.05, SUV_{max}: R² = 0.42, p < 0.05). The linear correlation between SUV-parameters and absorbed dose was weak (SUV_{mean}: R² = 0.25, p < 0.05, SUV_{max}: R² = 0.23, p < 0.05). The distribution of residuals of the data was deemed normal by visual inspection of the probability plots (Supplementary Figure S2).

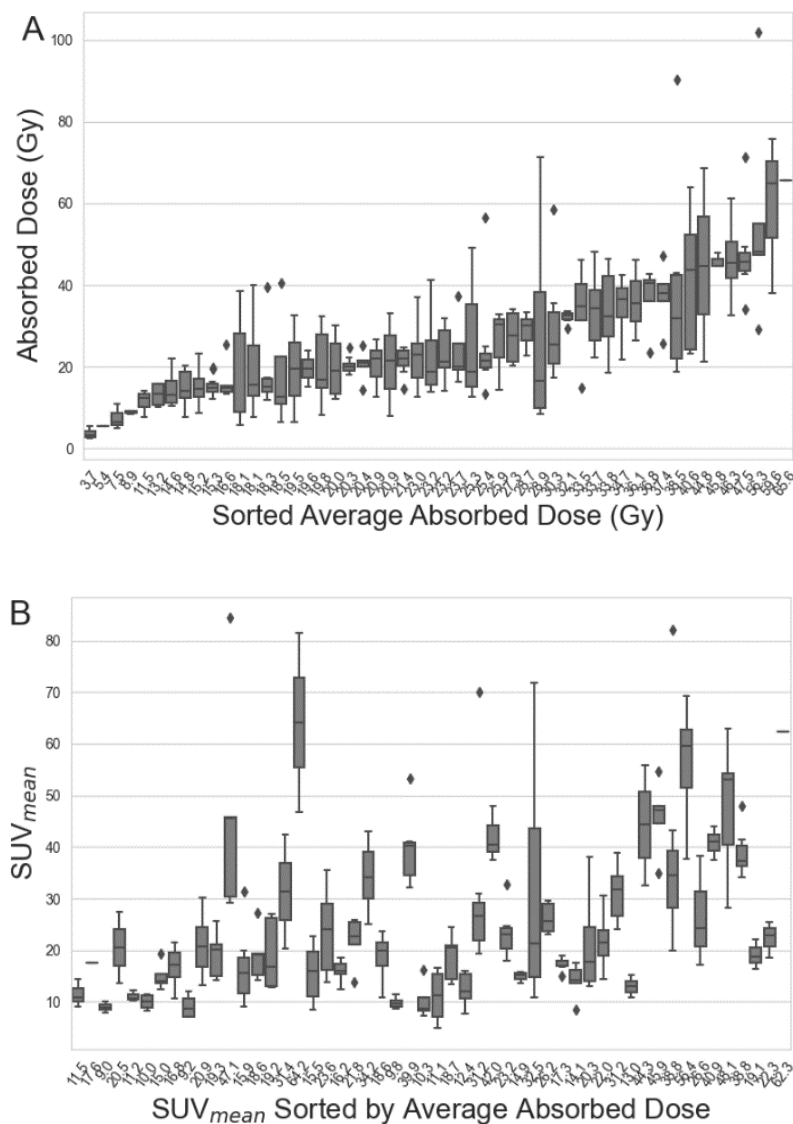


Figure 2. Box-and-whisker plots of [¹⁷⁷Lu]Lu-DOTA-TATE absorbed dose (A); and [⁶⁸Ga]Ga-DOTA-TOC SUV_{mean} (B), representing all the analysed tumours in each patient. The patients are sorted by average tumour-absorbed dose in both figures.

3.3. Absorbed Dose Prediction

A prediction model based on the linear correlation between SUV_{mean} and D/A_{adm} was explored. The mean absolute error and root mean squared error in the test-set was 1.33 and 1.77 Gy/GBq respectively. The R^2 -value of the test set was 0.24. Model parameters were $\alpha = 0.064$ and $\beta = 1.96$. The relative error (Δ_{AD}) between absorbed dose estimated by the prediction model (D_{pred}) and the actual absorbed dose is shown in Figure 4.

Using the population median absorbed dose, 23.3 Gy, as the cut-off point of a binary classifier, the predictive ability of the model was further tested. The performances of SUV_{mean} and SUV_{max} were comparable according to the ROC analysis (Figure 5).

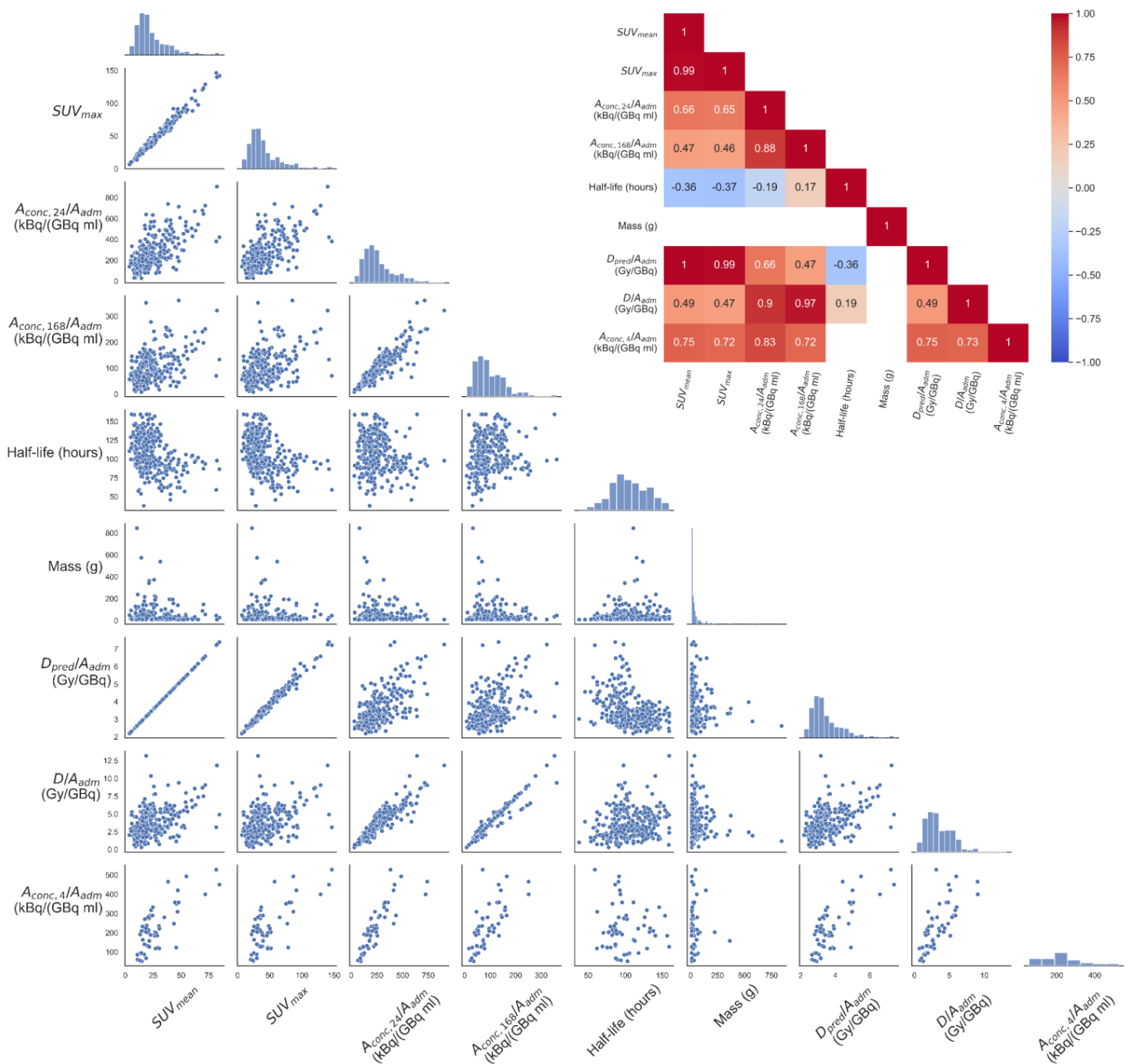


Figure 3. All parameters shown as scatter plots and their distribution on the diagonal. The inset heatmap shows the Pearson correlation coefficient where a significant linear correlation between parameters was found. The full data set is shown, and the predicted absorbed doses are based on the full data set.

3.4. Tumour Sub-Groups

None of the anatomical site groups showed significant inter-group differences. Grouping the tumours by SUV-values did reveal that a higher absorbed dose was observed in patients with higher SUV-values (Figure 6A). There were no statistical differences between tumours grouped by tumour mass. The results of the group analysis where an equal range of the parameters are used are found in Supplementary Figure S3.

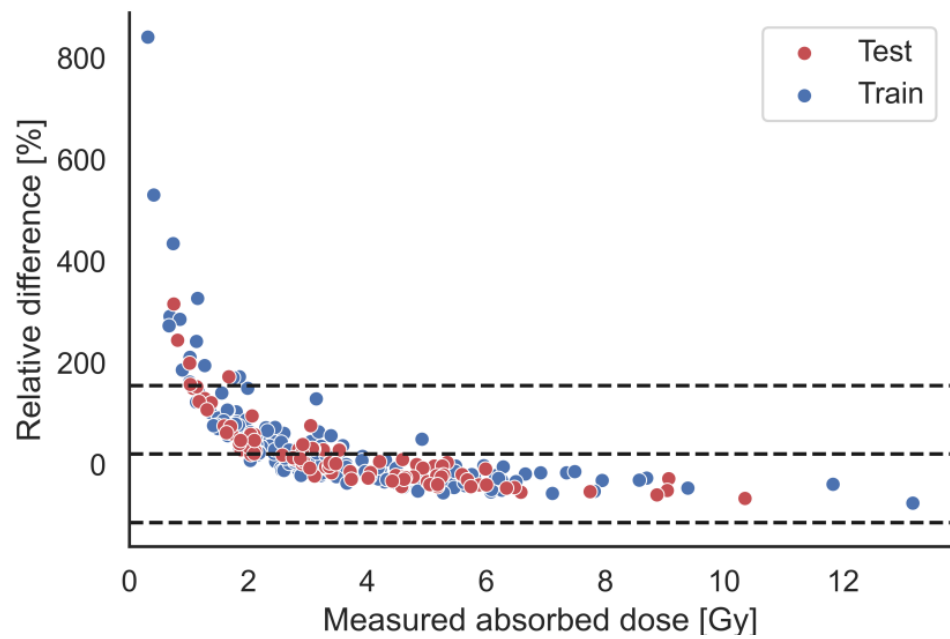


Figure 4. Relative error between predicted and calculated absorbed dose. The central dashed line is the average bias and the lower and upper 95% confidence intervals for the test are marked. Colours indicate whether the data point is from the training- or test-set. The predicted absorbed doses are calculated from parameters found in the training data set.

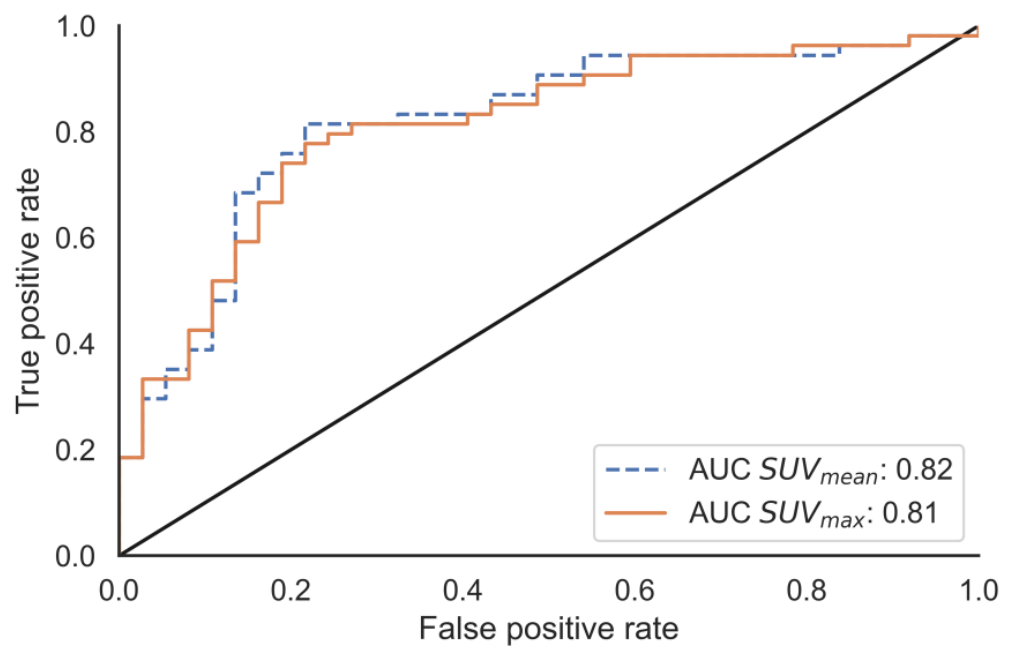


Figure 5. Receiver operating characteristic analysis. The ability to classify the absorbed dose as either above or below the test population median value of 3.0 Gy/GBq was tested.

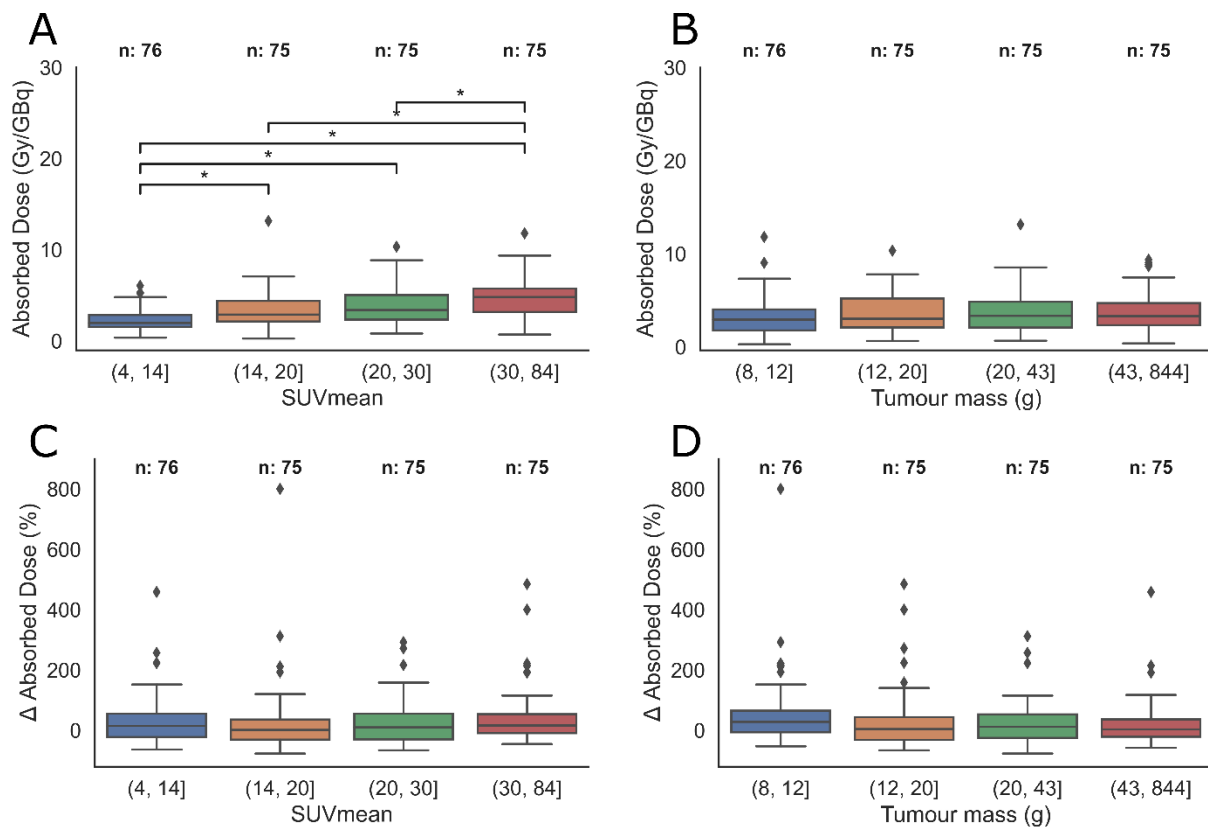


Figure 6. Differences of absorbed dose (A,B); and relative difference between predicted and calculated absorbed dose (C,D) between tumours grouped by SUV_{mean} and tumour mass. Grouping was done by keeping group sizes equal. Stars indicate significant differences of the group means (Tukey test). Only the absorbed dose of tumours grouped by SUV_{mean} was different between groups. A grouping based on equal ranges of mass and SUV_{mean}-values is found in the Supplementary Materials (Supplementary Figure S3).

4. Discussion

This retrospective study of 54 patients with GEP-NET found a weak albeit significant correlation between tumour specific uptake of [⁶⁸Ga]Ga-DOTA-TOC and [¹⁷⁷Lu]Lu-DOTA-TATE. There was a high inter- and inpatient variability in tumour measurements both for [⁶⁸Ga]Ga-DOTA-TOC and [¹⁷⁷Lu]Lu-DOTA-TATE. An absorbed dose prediction model based on SUV_{mean} was explored and assessed, showing that there could be a high deviation between predicted and actual absorbed dose, especially for tumours with lower absorbed doses.

Previous publications have reported median [⁶⁸Ga]Ga-DOTA-TOC SUV_{mean} for tumours ranging from approx. 10 to 25 and SUV_{max} ranging from approx. 20 to 40 [24,25,27,28], which is partly lower than our measurements. Slight variations may be due to differences in scanner performance, imaging acquisition (e.g., use of respiratory gating) and reconstruction settings. While delineation techniques will also be important for SUV_{mean}, this should not affect the SUV_{max} measurements. The absorbed dose previously found for [¹⁷⁷Lu]Lu-DOTA-TATE ranges from a few to 170 Gy [18–20,29–31] which is comparable to our measurements. It should be noted that some of the previous publications report on more or less heterogeneous groups of patients with regard to types of NET than those reported in the current work. Still, the overall result of our absorbed dose calculations is in agreement with the ones previously found in somatostatin-receptor expressing NETs.

As described in the introduction, a few studies have reported on attempts to correlate diagnostic and post therapeutic imaging of GEP-NETs. One group did a feasibility study on a small, mixed population and investigated SUV-parameters defined with a 40% threshold

on both [^{68}Ga]Ga-DOTA-TOC images and 24 h p.i. images of [^{177}Lu]Lu-DOTA-TATE [24]. They still found a significant but, commented by the authors, imperfect correlation. Another group looked at the correlation between PET-images of [^{68}Ga]Ga-DOTA-TOC and [^{177}Lu]Lu-Octreotate absorbed doses calculated from planar scans [25] of 61 tumours in 21 patients. They similarly found a significant but somewhat variable relationship between SUV_{mean} and absorbed dose. They argue that a “high SUV” (meaning $\text{SUV}_{\text{mean}} > 15$ and $\text{SUV}_{\text{max}} > 25$) could indicate a resulting “high dose range” of >10 Gy/GBq. The authors argued that caution had to be used as a considerable fraction of the “high” SUV tumours gave low absorbed doses. The group analysis in the current work shows the same tendencies, as a higher absorbed dose is associated with a higher SUV-value (Figure 6), but the large overlap of absorbed dose between SUV-groups still encourages caution. A limitation of the current study is the potential selection bias of only including tumours that could be clearly separated from adjacent tissues. While this probably results in more reliable measurements, and a broader range of tumours than selection of a predetermined number, especially tumours of low uptake may still be subjected to exclusion.

Our analysis show that absorbed dose from administration of [^{177}Lu]Lu-DOTA-TATE cannot be accurately predicted based on a single diagnostic scan of [^{68}Ga]Ga-DOTA-TOC performed in current clinical routine at our institution. A large intra- and interpatient variation was demonstrated by the high relative error variance, most notably for tumours of low absorbed dose where the predicted absorbed dose is highly overestimated (Figure 4). The cut-off at the population median absorbed dose was used as a starting point to explore a minimum ability for prediction. While the optimal cut-off value would be the absorbed dose that would classify the treatment as successful, this value is not firmly established. The median was therefore selected as a robust parameter, so the results could be compared with other tumour populations, as variations in methodology between centres will probably not affect the median to a large degree. Although SUV_{mean} was used in the current analyses, an argument can be made for the use of SUV_{max} as, although being sensitive to image noise, this parameter is virtually independent of the segmentation technique and is simple to define. In the current work, it was also shown to be highly correlated with SUV_{mean} (Figure 3), and while SUV_{mean} 's similar interpretation to $A_{\text{conc},24}/A_{\text{adm}}$ resulted in its use, the results would be highly similar for SUV_{max} .

The absorbed-dose calculation that represents the ground truth in this work is primarily based on two parameters; the effective half-life for the mono-exponential wash-out phase, and the [^{177}Lu]Lu-DOTA-TATE activity concentrations. The PRRT absorbed dose was highly correlated to the [^{177}Lu]Lu-DOTA-TATE activity concentration at 24 and 168 h p.i., but considerably less correlated with the effective half-life after 24 h (Figure 3). Interestingly, the SUV_{mean} was negatively associated with the effective half-life of [^{177}Lu]Lu-DOTA-TATE, and this relationship was actually also stronger than the one between effective half-life and absorbed dose. This leads to the systematic trend in Figure 4, which may make it appear as though a non-linear model would have been better suited for the prediction model. The negative association between SUV_{mean} and effective half-life of [^{177}Lu]Lu-DOTA-TATE could be due to biological, or even radiobiological, factors and would be interesting to pursue in further studies. While the SUV_{mean} was positively correlated with [^{177}Lu]Lu-DOTA-TATE activity concentration at 24 and 168 h p.i. (Figure 3), for a subpopulation of the patients a SPECT/CT at 4 h was also obtained, and the $A_{\text{conc},4}/A_{\text{adm}}$ had an even better correlation with SUV_{mean} . This indicates that the delay between administration and image acquisition for [^{68}Ga]Ga-DOTA-TOC and [^{177}Lu]Lu-DOTA-TATE can possibly explain the poor linear correlation between SUV_{mean} of [^{68}Ga]Ga-DOTA-TOC and $A_{\text{conc},24}/A_{\text{adm}}$ of [^{177}Lu]Lu-DOTA-TATE, and hence partly also the absorbed dose deviation. Furthermore, it can be considered whether a dose prediction model should include a separate term describing an association between SUV_{mean} and effective half-life of [^{177}Lu]Lu-DOTA-TATE. It should also be pointed out that there may be various patient- or tumour-specific factors, not investigated in this work, that could also be incorporated in order to form an improved prediction model.

The SPECTs obtained indicate that 168 h p.i. is a better time point for single time point tumour dosimetry than 24 h p.i. (R^2 -value of 0.82 and 0.94 for $A_{conc,24}/A_{adm}$ and $A_{conc,168}/A_{adm}$ respectively), in agreement with previous investigations [32,33]. Still, the possibility for delayed 24 h imaging of a PET tracer (possibly using another radionuclide) can prove fruitful for continued investigations.

5. Conclusions

There was a high inter- and intra-patient variability in tumour measurements both for [^{68}Ga]Ga-DOTA-TOC and [^{177}Lu]Lu-DOTA-TATE. While a significant correlation between tumour-specific uptake of [^{68}Ga]Ga-DOTA-TOC and [^{177}Lu]Lu-DOTA-TATE absorbed dose was found for individual tumours, the correlation was noisy, and the absorbed-dose prediction model based on SUV_{mean} should be used with care depending on the purpose and required accuracy.

Supplementary Materials: The following supporting information can be downloaded at: <https://www.mdpi.com/article/10.3390/cancers15041134/s1>, Figure S1: An Esser phantom with spherical inserts of 2, 4, 8, 16 and 113 mL was used to determine threshold and recovery coefficients; Figure S2: Probability plots of the residuals of the predicted and calculated absorbed dose from SUV_{mean} (A) and SUV_{max} (B); Figure S3: The group analysis with equal group size instead of equal range in grouping parameters. Stars indicate statistically significant differences of the group means according to the Tukey-test.

Author Contributions: C.S., L.T.M., J.B. conceived and designed the study. R.B. performed the segmentations, with supervision from J.C., R.B. analysed the data, with contributions and supervision from J.B. All authors interpreted the data. R.B. wrote the manuscript, with contributions from J.B. and C.S. All authors have read and agreed to the published version of the manuscript.

Funding: This research received no external funding.

Institutional Review Board Statement: The study was conducted in accordance with the Declaration of Helsinki, and was approved by the local data protection officer at Oslo University Hospital (20/18797, date: 3 September 2020).

Informed Consent Statement: Patient consent was waived by the local data protection officer at Oslo University Hospital due to the study being approved as a quality assurance study.

Data Availability Statement: The datasets generated during and/or analysed during the current study are available from the corresponding author on request.

Conflicts of Interest: The authors declare no conflict of interest.

References

1. Cives, M.; Strosberg, J.R. Gastroenteropancreatic Neuroendocrine Tumors. *CA A Cancer J. Clin.* **2018**, *68*, 471–487. [[CrossRef](#)]
2. Meeker, A.; Heaphy, C. Gastroenteropancreatic endocrine tumors. *Mol. Cell. Endocrinol.* **2014**, *386*, 101–120. [[CrossRef](#)]
3. Papotti, M.; Bongiovanni, M.; Volante, M.; Allia, E.; Landolfi, S.; Helboe, L.; Schindler, M.; Cole, S.L.; Bussolati, G. Expression of somatostatin receptor types 1-5 in 81 cases of gastrointestinal and pancreatic endocrine tumors. A correlative immunohistochemical and reverse-transcriptase polymerase chain reaction analysis. *Virchows Arch.* **2002**, *440*, 461–475. [[CrossRef](#)]
4. Baumann, T.; Rottenburger, C.; Nicolas, G.; Wild, D. Gastroenteropancreatic neuroendocrine tumours (GEP-NET)—Imaging and staging. *Best Pract. Res. Clin. Endocrinol. Metab.* **2016**, *30*, 45–57. [[CrossRef](#)]
5. Camus, B.; Cottreau, A.S.; Palmieri, L.J.; Dermine, S.; Tenenbaum, F.; Brezault, C.; Coriat, R. Indications of Peptide Receptor Radionuclide Therapy (PRRT) in Gastroenteropancreatic and Pulmonary Neuroendocrine Tumors: An Updated Review. *J. Clin. Med.* **2021**, *10*, 1267. [[CrossRef](#)] [[PubMed](#)]
6. Antunes, P.; Ginj, M.; Zhang, H.; Waser, B.; Baum, R.P.; Reubi, J.C.; Maecke, H. Are radiogallium-labelled DOTA-conjugated somatostatin analogues superior to those labelled with other radiometals? *Eur. J. Nucl. Med. Mol. Imaging* **2007**, *34*, 982–993. [[CrossRef](#)] [[PubMed](#)]
7. Hope, T.A.; Bergsland, E.K.; Bozkurt, M.F.; Graham, M.; Heaney, A.P.; Herrmann, K.; Howe, J.R.; Kulke, M.H.; Kunz, P.L.; Mailman, J.; et al. Appropriate Use Criteria for Somatostatin Receptor PET Imaging in Neuroendocrine Tumors. *J. Nucl. Med.* **2018**, *59*, 66–74. [[CrossRef](#)]

8. Kwekkeboom, D.J.; Kam, B.L.; van Essen, M.; Teunissen, J.J.; van Eijck, C.H.; Valkema, R.; de Jong, M.; de Herder, W.W.; Krenning, E.P. Somatostatin-receptor-based imaging and therapy of gastroenteropancreatic neuroendocrine tumors. *Endocr. Relat. Cancer* **2010**, *17*, R53–R73. [[CrossRef](#)] [[PubMed](#)]
9. Soydal, Ç.; Peker, A.; Özkan, E.; Küçük, Ö.N.; Kir, M.K. The role of baseline Ga-68 DOTATATE positron emission tomography/computed tomography in the prediction of response to fixed-dose peptide receptor radionuclide therapy with Lu-177 DOTATATE. *Turk. J. Med. Sci.* **2016**, *46*, 409–413. [[CrossRef](#)]
10. Poeppel, T.D.; Binse, I.; Petersenn, S.; Lahner, H.; Schott, M.; Antoch, G.; Brandau, W.; Bockisch, A.; Boy, C. 68Ga-DOTATOC versus 68Ga-DOTATATE PET/CT in functional imaging of neuroendocrine tumors. *J. Nucl. Med.* **2011**, *52*, 1864–1870. [[CrossRef](#)]
11. Das, S.; Al-Toubah, T.; El-Haddad, G.; Strosberg, J. (177)Lu-DOTATATE for the treatment of gastroenteropancreatic neuroendocrine tumors. *Expert Rev. Gastroenterol. Hepatol.* **2019**, *13*, 1023–1031. [[CrossRef](#)] [[PubMed](#)]
12. Bodei, L.; Mueller-Brand, J.; Baum, R.P.; Pavel, M.E.; Hörsch, D.; O’Dorisio, M.S.; O’Dorisio, T.M.; Howe, J.R.; Cremonesi, M.; Kwekkeboom, D.J.; et al. The joint IAEA, EANM, and SNMMI practical guidance on peptide receptor radionuclide therapy (PRRT) in neuroendocrine tumours. *Eur. J. Nucl. Med. Mol. Imaging* **2013**, *40*, 800–816. [[CrossRef](#)] [[PubMed](#)]
13. Kim, S.J.; Pak, K.; Koo, P.J.; Kwak, J.J.; Chang, S. The efficacy of (177)Lu-labelled peptide receptor radionuclide therapy in patients with neuroendocrine tumours: A meta-analysis. *Eur. J. Nucl. Med. Mol. Imaging* **2015**, *42*, 1964–1970. [[CrossRef](#)] [[PubMed](#)]
14. Kwekkeboom, D.J.; de Herder, W.W.; Kam, B.L.; van Eijck, C.H.; van Essen, M.; Kooij, P.P.; Feelders, R.A.; van Aken, M.O.; Krenning, E.P. Treatment with the radiolabeled somatostatin analog [177 Lu-DOTA 0,Tyr3]octreotate: Toxicity, efficacy, and survival. *J. Clin. Oncol.* **2008**, *26*, 2124–2130. [[CrossRef](#)]
15. Strosberg, J.; El-Haddad, G.; Wolin, E.; Hendifar, A.; Yao, J.; Chasen, B.; Mittra, E.; Kunz, P.L.; Kulke, M.H.; Jacene, H.; et al. Phase 3 Trial of (177)Lu-Dotatate for Midgut Neuroendocrine Tumors. *New Engl. J. Med.* **2017**, *376*, 125–135. [[CrossRef](#)]
16. Cives, M.; Strosberg, J. Radionuclide Therapy for Neuroendocrine Tumors. *Curr. Oncol. Rep.* **2017**, *19*, 9. [[CrossRef](#)]
17. Sjogreen Gleisner, K.; Chouin, N.; Gabina, P.M.; Cicone, F.; Gnesin, S.; Stokke, C.; Konijnenberg, M.; Cremonesi, M.; Verburg, F.A.; Bernhardt, P.; et al. EANM dosimetry committee recommendations for dosimetry of 177Lu-labelled somatostatin-receptor- and PSMA-targeting ligands. *Eur. J. Nucl. Med. Mol. Imaging* **2022**, *49*, 1778–1809. [[CrossRef](#)]
18. Ilan, E.; Sandström, M.; Wassberg, C.; Sundin, A.; Garske-Román, U.; Eriksson, B.; Granberg, D.; Lubberink, M. Dose response of pancreatic neuroendocrine tumors treated with peptide receptor radionuclide therapy using 177Lu-DOTATATE. *J. Nucl. Med.* **2015**, *56*, 177–182. [[CrossRef](#)]
19. Roth, D.; Gustafsson, J.R.; Warfvinge, C.F.; Sundlöv, A.; Åkesson, A.; Tennvall, J.; Sjogreen Gleisner, K. Dosimetric quantities of neuroendocrine tumors over treatment cycles with (177)Lu-DOTA-TATE. *J. Nucl. Med.* **2022**, *63*, 399–405. [[CrossRef](#)]
20. Wehrmann, C.; Senfleben, S.; Zachert, C.; Müller, D.; Baum, R.P. Results of individual patient dosimetry in peptide receptor radionuclide therapy with 177Lu DOTA-TATE and 177Lu DOTA-NOC. *Cancer Biother. Radiopharm.* **2007**, *22*, 406–416. [[CrossRef](#)]
21. Reubi, J.C.; Schär, J.C.; Waser, B.; Wenger, S.; Heppeler, A.; Schmitt, J.S.; Mäcke, H.R. Affinity profiles for human somatostatin receptor subtypes SST1–SST5 of somatostatin radiotracers selected for scintigraphic and radiotherapeutic use. *Eur. J. Nucl. Med.* **2000**, *27*, 273–282. [[CrossRef](#)] [[PubMed](#)]
22. Velikyan, I.; Sundin, A.; Sörensen, J.; Lubberink, M.; Sandström, M.; Garske-Román, U.; Lundqvist, H.; Granberg, D.; Eriksson, B. Quantitative and qualitative inpatient comparison of 68Ga-DOTATOC and 68Ga-DOTATATE: Net uptake rate for accurate quantification. *J. Nucl. Med.* **2014**, *55*, 204–210. [[CrossRef](#)] [[PubMed](#)]
23. Esser, J.P.; Krenning, E.P.; Teunissen, J.J.; Kooij, P.P.; van Gameren, A.L.; Bakker, W.H.; Kwekkeboom, D.J. Comparison of [(177)Lu-DOTA(0),Tyr(3)]octreotate and [(177)Lu-DOTA(0),Tyr(3)]octreotide: Which peptide is preferable for PRRT? *Eur. J. Nucl. Med. Mol. Imaging* **2006**, *33*, 1346–1351. [[CrossRef](#)]
24. Thuillier, P.; Maajem, M.; Schick, U.; Blanc-Beguín, F.; Hennebicq, S.; Metges, J.P.; Salaun, P.Y.; Kerlan, V.; Bourhis, D.; Abgral, R. Clinical Assessment of 177Lu-DOTATATE Quantification by Comparison of SUV-Based Parameters Measured on Both Post-PRRT SPECT/CT and 68Ga-DOTATOC PET/CT in Patients With Neuroendocrine Tumors: A Feasibility Study. *Clin. Nucl. Med.* **2021**, *46*, 111–118. [[CrossRef](#)]
25. Ezziddin, S.; Lohmar, J.; Yong-Hing, C.J.; Sabet, A.; Ahmadzadehfar, H.; Kukuk, G.; Biersack, H.J.; Guhlke, S.; Reichmann, K. Does the pretherapeutic tumor SUV in 68Ga DOTATOC PET predict the absorbed dose of 177Lu octreotate? *Clin. Nucl. Med.* **2012**, *37*, e141–e147. [[CrossRef](#)] [[PubMed](#)]
26. Eckerman, K.; Endo, A. ICRP Publication 107. Nuclear decay data for dosimetric calculations. *Ann. ICRP* **2008**, *38*, 7–96.
27. Kratochwil, C.; Stefanova, M.; Mavriopoulou, E.; Holland-Letz, T.; Dimitrakopoulou-Strauss, A.; Afshar-Oromieh, A.; Mier, W.; Haberkorn, U.; Giesel, F.L. SUV of [68Ga]DOTATOC-PET/CT Predicts Response Probability of PRRT in Neuroendocrine Tumors. *Mol. Imaging Biol.* **2015**, *17*, 313–318. [[CrossRef](#)]
28. Thuillier, P.; Bourhis, D.; Metges, J.P.; Le Pennec, R.; Amrane, K.; Schick, U.; Blanc-Beguín, F.; Hennebicq, S.; Salaun, P.Y.; Kerlan, V.; et al. Prospective study of dynamic whole-body 68Ga-DOTATOC-PET/CT acquisition in patients with well-differentiated neuroendocrine tumors. *Sci. Rep.* **2021**, *11*, 4727. [[CrossRef](#)]
29. Jahn, U.; Ilan, E.; Sandström, M.; Garske-Román, U.; Lubberink, M.; Sundin, A. 177Lu-DOTATATE Peptide Receptor Radionuclide Therapy: Dose Response in Small Intestinal Neuroendocrine Tumors. *Neuroendocrinology* **2020**, *110*, 662–670. [[CrossRef](#)]
30. Jahn, U.; Ilan, E.; Sandström, M.; Lubberink, M.; Garske-Román, U.; Sundin, A. Peptide Receptor Radionuclide Therapy (PRRT) with (177)Lu-DOTATATE.; Differences in Tumor Dosimetry, Vascularity and Lesion Metrics in Pancreatic and Small Intestinal Neuroendocrine Neoplasms. *Cancers* **2021**, *13*, 962. [[CrossRef](#)]

31. Kupitz, D.; Wetz, C.; Wissel, H.; Wedel, F.; Apostolova, I.; Wallbaum, T.; Ricke, J.; Amthauer, H.; Grosser, O.S. Software-assisted dosimetry in peptide receptor radionuclide therapy with ¹⁷⁷Lutetium-DOTATATE for various imaging scenarios. *PLoS ONE* **2017**, *12*, e0187570. [[CrossRef](#)] [[PubMed](#)]
32. Hanscheid, H.; Lapa, C.; Buck, A.K.; Lassmann, M.; Werner, R.A. Dose Mapping After Endoradiotherapy with (¹⁷⁷)Lu-DOTATATE/DOTATOC by a Single Measurement after 4 Days. *J. Nucl. Med.* **2018**, *59*, 75–81. [[CrossRef](#)] [[PubMed](#)]
33. Chicheportiche, A.; Sason, M.; Godefroy, J.; Krausz, Y.; Zidan, M.; Oleinikov, K.; Meirovitz, A.; Gross, D.J.; Grozinsky-Glasberg, S.; Ben-Haim, S. Simple model for estimation of absorbed dose by organs and tumors after PRRT from a single SPECT/CT study. *EJNMMI Phys.* **2021**, *8*, 63. [[CrossRef](#)] [[PubMed](#)]

Disclaimer/Publisher's Note: The statements, opinions and data contained in all publications are solely those of the individual author(s) and contributor(s) and not of MDPI and/or the editor(s). MDPI and/or the editor(s) disclaim responsibility for any injury to people or property resulting from any ideas, methods, instructions or products referred to in the content.